

## The Contribution of Lake Enhancement to Extreme Snowfall within the Chicago–Milwaukee Urban Corridor during the 2011 Groundhog Day Blizzard

NATHAN D. OWENS, ROBERT M. RAUBER, BRIAN F. JEWETT, AND GREG M. MCFARQUHAR

*Department of Atmospheric Sciences, University of Illinois at Urbana–Champaign, Urbana, Illinois*

(Manuscript received 6 February 2017, in final form 19 March 2017)

### ABSTRACT

This paper examines the impact of the Laurentian Great Lakes (GL) on atmospheric structure, stability, and precipitation within the Chicago–Milwaukee urban corridor during the passage of the 1–2 February 2011 extratropical cyclone. This storm produced the third largest snowfall [53.8 cm (21.2 in.)] recorded in a 130-yr period in the city of Chicago. Two simulations of the storm using the Weather Research and Forecasting (WRF) Model are described: the first with the GL present, and the second with the lakes replaced with land having characteristics of adjacent shores.

The GL were found to alter the surface temperature and moisture fields in their lee during cyclone passage. The changes were limited to the layer below the frontal inversion, but were significant enough to reduce the mean sea level pressure in some locations by 2.0–2.5 hPa, and raise the surface temperature and dewpoint temperature by 2°–4°C across several states downwind. In the Chicago–Milwaukee metropolitan corridor where the heavy snow occurred, the surface temperature and dewpoint temperature increased from +3° to +6°C as a result of heating and moistening of the lower atmosphere by the GL. Enhanced convergence also occurred along the downwind shoreline. Despite these changes, the areal impact on precipitation was surprisingly small, with liquid equivalent precipitation increases exceeding 5 mm limited to a small area over metropolitan Chicago late in the storm. The reason for the limited impact appeared to be the shallow nature of the cold air mass below the frontal inversion. Nevertheless, over metropolitan Chicago, as much as 20% of the snowfall could be attributed to the presence of the GL.

### 1. Introduction

The Chicago metropolitan area has the third largest urban population in the United States. Combined with the adjacent Milwaukee metropolitan area, the total 2014 population along the western shore of Lake Michigan, based on U.S. census estimates, exceeds 11 million. Winter snowstorms are common across this region, but disastrous snowstorms with accumulations exceeding 40 cm (~16 in.) occur on average less than once per decade over the last century (Table 1). The most extreme snowfall events occur when deep low pressure centers associated with extratropical cyclones pass across Illinois, just south of Lake Michigan, so that the comma heads of the storms are located over the lake. In this scenario, low-level airflow across Lake Michigan is northeasterly, leading to the possibility that the flux of moisture and heat from Lake Michigan, and potentially from Lake Huron upstream, may enhance the overall

snowfall within the Chicago–Milwaukee corridor. Such an extreme event occurred on 1–2 February 2011. The storm, colloquially referred to as the “Groundhog Day Blizzard,” produced the third highest snowfall recorded in Chicago [53.8 cm (21.2 in.)] and blizzard conditions that shut down much of the Chicago urban corridor for days. The storm produced a swath of heavy snowfall, the axis of which extended from northeastern Oklahoma through Chicago, and northeastward into Ontario, Canada (Fig. 1), with the highest snowfall totals recorded along the Chicago–Milwaukee urban corridor.

To date, four studies have been published investigating aspects of the 1–2 February storm, although none investigated the heavy snowfall. Ikeda et al. (2013) evaluated the quality of High-Resolution Rapid Refresh (HRRR) model simulations of this storm and other cold-season cyclones, concluding that the HRRR model reliably forecasts precipitation amount and extent in the cold season. Thompson and Eidhammer (2014) described implementation, testing, and results of a newly modified Thompson bulk microphysical parameterization within

Corresponding author: Robert M. Rauber, r-rauber@illinois.edu

TABLE 1. Worst snowstorms at Chicago<sup>a</sup> (Source: [National Weather Service 2015](#)). Boldface indicates the period of interest for our study.

Worst snowstorms in Chicago history	Amounts
25–27 Jan 1967	58.4 cm (23.0 in.)
1–3 Jan 1999	54.9 cm (21.6 in.)
<b>31 Jan–2 Feb 2011</b>	<b>53.8 cm (21.2 in.)</b>
12–14 Jan 1979	51.6 cm (20.3 in.)
31 Jan–2 Feb 2015	49.0 cm (19.3 in.)
25–26 Mar 1930	48.8 cm (19.2 in.)
7–8 Mar 1931	41.1 cm (16.2 in.)
30 Jan 1939	37.8 cm (14.9 in.)
6–7 Jan 1918	37.8 cm (14.9 in.)
17–19 Dec 1929	37.6 cm (14.8 in.)

<sup>a</sup> Official snowfall observations began in the 1885/86 winter and were taken at a number of sites in the downtown area. From July 1905 to 1925 they were made at the U.S. Court House, and from January 1926 to 20 June 1942 they were made at the University of Chicago. The official site was Midway Airport between 20 June 1942 and 16 January 1980. Since that time, the official site has been O'Hare International Airport.

the Weather Research and Forecasting (WRF) Model, using the 1–2 February storm as the framework for testing the new parameterization. [Rauber et al. \(2014\)](#) examined the source of lightning discharges within the comma head of the storm, demonstrating that lightning within the snowstorm was associated with elevated convection on the south side of the comma head. Subsequently, [Warner et al. \(2014\)](#) showed that cloud-to-ground lightning strikes within the comma head of this storm almost exclusively struck tall towers.

A number of studies have investigated the impact of the Laurentian Great Lakes (GL) on cyclone structure, but none to date have focused specifically on lake enhancement of snowfall during a cyclone passage. The earliest study to question the influence of the GL on cyclone structure was that of [Cox \(1917\)](#), who argued that GL heat fluxes should cause low pressure systems to occur more frequently and have greater energy. [Petterssen \(1956\)](#), p. 326 expanded on Cox's idea, arguing that GL heat fluxes should accelerate a cyclone's movement into, and delay its departure from the region, effectively causing storms to linger over the GL. [Petterssen and Calabrese \(1959\)](#) also showed that heating by the GL could lower surface pressure by as much as 6–7 hPa. [Angel and Isard's \(1997\)](#) climatology of speed and intensity changes of cyclones over the GL provides support for [Cox \(1917\)](#) and [Petterssen's \(1956\)](#) arguments. The first numerical studies of GL impacts on cyclone structure, reported by [Danard and Rao \(1972\)](#), [Danard and McMillan \(1974\)](#), and [Neralla and Danard \(1975\)](#), found that GL heat fluxes can induce 1000-hPa height reductions as large as 70 m and boundary layer

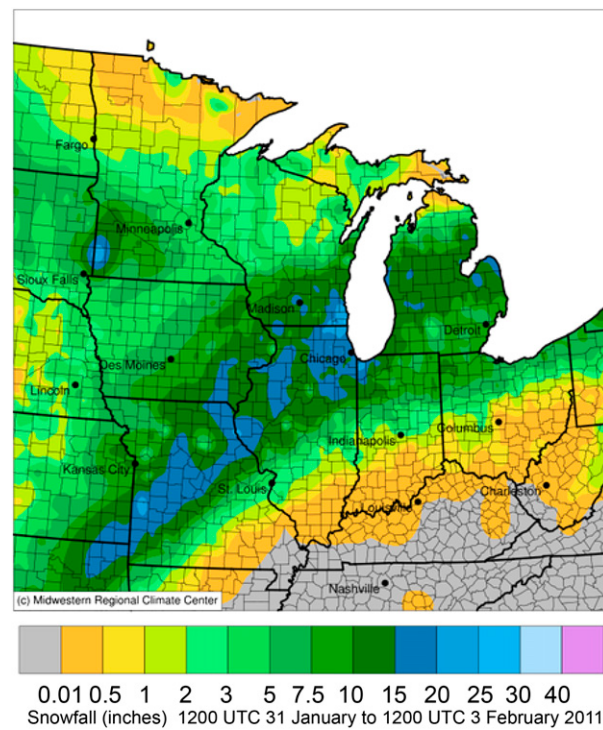


FIG. 1. Total snow accumulation during the passage of the 1–2 Feb 2011 cyclone.

temperature rises as large as 7°C. [Sousounis and Shirer \(1992\)](#), [Sousounis and Fritsch \(1994\)](#), [Sousounis \(1997, 1998\)](#), and [Sousounis and Mann \(2000\)](#) further showed that heat fluxes over the GL can alter cyclone structure and evolution immediately downstream of GL region. Beyond these studies, little work has been done to date to understand possible influences of the GL on winter cyclones. We are unaware of any studies that specifically examine the impact of the GL on precipitation *during* cyclone passage.

Although not focused on cyclones, recent studies have examined the impact of ice cover on precipitation associated with lake-effect snowstorms that typically occur in a cyclone's wake. [Wright et al. \(2013\)](#), for example, explored the sensitivity of lake-effect snowfall to changes in lake ice cover and surface temperature. They found that the spatial pattern of unfrozen lake surfaces determines the distribution of lake-effect snowfall, and that complete ice cover eliminates lake-effect snow. [Vavrus et al. \(2013\)](#) imposed 100% ice coverage on the GL (individually and entirely) in multidecadal regional climate model simulations, finding downwind snowfall reductions, particularly for Lakes Superior and Michigan. They found that precipitable water and low-level clouds decreased and downstream pressure increased when the lake surfaces were frozen. They also noted that reduced

wind speed over the lakes limited shoreline convergence when the lakes were frozen, further minimizing downwind precipitation. [Gerbush et al. \(2008\)](#) analyzed the energy fluxes above ice-covered lakes, as measured during the Great Lakes Ice Cover-Atmospheric Flux (GLICAF) experiment. They found the temperature difference between the air and sea surface to have a greater impact on sensible heat flux than that of the wind speed, though both were important. [Cordeira and Laird \(2008\)](#) found a significant influence on energy fluxes related to the thickness of ice cover; when a lake was iced over, lake-effect precipitation could still occur if the ice was not thick enough to substantially inhibit energy transfer.

This paper examines the impact of the GL on atmospheric structure, stability, and precipitation production along the urban corridor on the west side of Lake Michigan during the passage of the 1–2 February cyclone over the GL. Northeasterly flow persisted across the upper GL for nearly 18 h during the period of cyclone-induced heavy snowfall associated with the passage of the storm across the GL. This raises the possibility that lake enhancement of snowfall may have occurred along the western and southern shorelines of Lake Michigan, particularly across the Chicago, Illinois–Milwaukee, Wisconsin, urban corridor where near-record snowfall was observed. Herein, we use numerical model simulations to test the hypothesis that the northeasterly flow across the GL during the 1–2 February cyclone had a significant impact on the extreme snowfall in the Chicago–Milwaukee corridor during this event. Two simulations of this storm using the WRF Model are described: the first with the GL present, and the second with the GL replaced with land having characteristics of adjacent shores. Quantitative comparisons of these simulations were used to determine the influence of the GL on atmospheric structure, stability, and precipitation production along the urban corridor as the cyclone traversed the region. The overall goal of this study is to quantify the impact of the GL on snowfall within the urban corridor during this event.

## 2. Methodology

To address the hypothesis stated above, two WRF Model simulations were carried out for the 1–2 February 2011 cyclone: the first with the GL present [hereafter labeled “with lakes” (WL)] and the second with the GL replaced with land having characteristics of nearby shores [hereafter labeled “no lakes” (NL)]. Differences between the simulations were used to diagnose and understand the roles of the GL in precipitation production within the urban corridor. The approach of replacing the



FIG. 2. The 9-km outer domain and 3-km inner domain for the WRF simulations.

lakes with the natural conditions found on nearby shores has previously been applied by [Sousounis and Fritsch \(1994\)](#) and [Notaro et al. \(2013\)](#). [Sousounis and Fritsch \(1994\)](#) examined the development of a mesoscale vortex downstream of the GL following the onset of a cold air outbreak. [Notaro et al. \(2013\)](#) investigated the impacts of the GL on seasonal climate of the region, rather than on structural changes associated with a single extreme event.

The WRF simulations were run from 0000 UTC 1 February to 1500 UTC 2 February 2011. The initial and boundary condition grids were taken from the 12-km National Centers for Environmental Prediction (NCEP) North American Mesoscale Forecast System (NAM), using a combination of analyses (every 6 h) and forecasts (at 3 h between analyses). The simulations were initialized 20 h prior to the arrival of the cyclone’s precipitation shield at the south end of Lake Michigan. WRF-ARW version 3.7 was used. Two domains (two-way nesting) were employed, with 9-km grid spacing on the outer domain and 3 km on the inner nest (Fig. 2) and 90 vertical levels. In the NL simulation, the lakes were removed in both domains.

Treatment of physical processes used the following parameterizations: surface layer based on Monin–Obukhov similarity theory ([Jiménez et al. 2012](#)), unified Noah land surface scheme ([Chen and Dudhia 2001](#)),

the Yonsei University (YSU; Hong et al. 2006) planetary boundary layer, RRTM for GCMs (RRTMG) shortwave and longwave radiation (Iacono et al. 2008), and Morrison double-moment microphysics (Morrison et al. 2009). Our goal was to have a WL control simulation that, as closely as possible, reproduced the observed storm. Early tests we did with different microphysics and surface schemes available in WRF produced cyclones with evolution that departed more from the observed storm in either location or intensity of the central low pressure. The choices used for the WL simulation produced a simulation closest to the observed behavior of the storm from which we could evaluate the role of the lakes. For the WL simulation, the lakes, and ice cover on the lakes as present at the time of the event, were retained in the model. For the NL simulation, the lakes, both the water- and ice-covered portions, were replaced with land.

The Great Lakes were replaced on both grids with characteristics of nearby land in the NL experiment. Owens (2016) describes the procedure for replacement of the lakes in the WRF Model. A brief summary is provided here. All water surfaces in an area between latitudes  $41.35^{\circ}$  and  $49.02^{\circ}\text{N}$ , and longitudes  $76.05^{\circ}$  and  $92.30^{\circ}\text{W}$  were converted to a land surface. This conversion required changes in a number of input parameters. The binary masks that distinguish between water and land were converted to land. A second mask deals specifically with ice on water bodies. During the storm, Lake Erie was entirely ice covered, as well as parts of Lake Huron. Other lakes had ice on their peripheries. The ice mask was reset to land surface. Land use was then set to have characteristics of the nearby shore (e.g., deciduous broadleaf forest; mixed forest; dryland, cropland, and pasture; mixed forest; or cropland/grassland mosaic). The land-use boundaries were set to match the surrounding land to a close approximation. The skin temperature of the lakes, including ice-covered regions, was set to values of nearby land. This led to colder surfaces, since the lakes were warmer than the shores. Soil temperatures had to be introduced since soil replaced the water. Soil temperatures, and moisture, were set at specific depths (0–10, 10–40, 40–100, and 100–200 cm) with values matching nearby shores. Snow cover was present across the region from previous events. Snow was added to the land that replaced the lakes in order to maintain consistency with surrounding areas. Snow depth and albedo were specified corresponding to nearby shoreline values. Soil category was also adjusted to values of the adjacent shorelines. Soil categories were assigned 25% coverage for each of the soil types common in the Great Lakes region. Monthly surface albedo and green fraction, the subgrid

proportion of each cell that is covered in foliage for each month, were also given shoreline values appropriate for February. Topography, however, was not changed. Though the lakes were removed, their surfaces were kept flat. Other parameters related to topography, such as various orographic asymmetry parameters, were also left unchanged.

Although the lakes were replaced, the characteristics of the atmosphere above the lakes were left unchanged in the initialization fields. There was a 20-h period in the simulation prior to the arrival of the cyclone. In the WL simulation, this time allowed a lake-induced boundary layer to develop, as would exist when, in nature, the cyclone approached the GL. In the NL simulation, the 20-h period allowed any potential effect of the GL present in the initial conditions to be advected out of the GL region prior to the arrival of the northern periphery of the precipitation shield accompanying the cyclone. The time period of 20 h was determined to be sufficient for low-level air to depart the lakes region based on the values of the surface winds, as well as careful examination of fields influenced by the lakes, such as low-level relative humidity. Several simulations with initial start times were conducted to determine the best start time to achieve these common goals, and to have the cyclone evolve as closely as possible in the WL simulation to the true cyclone evolution. The simulation starting 20 h before precipitation arrival at the Chicago–Milwaukee corridor best met all these requirements.

### 3. Comparison of the observed 1–2 February 2011 cyclone with the WL simulation

The WL simulation serves as the control simulation in this study. It is important, therefore, that the WL simulation reasonably reproduces characteristics of the actual cyclone, including the precipitation distribution, particularly in the vicinity of the GL. Figures 3a and 3c show the observed sea level pressure and composite radar reflectivity at 0000 UTC 2 February and 0600 UTC 2 February, bridging the period of heaviest snowfall when half of the total snow accumulation occurred in the Chicago–Milwaukee corridor. Figures 3b and 3d show the same parameters at the same valid times from the WL simulation at 24 and 30 h. The verification sea level pressure field in Figs. 3a and 3c (and the 300- and 850-hPa charts depicting the verification upper-tropospheric flows in Figs. 4a and 4c) were obtained from the initialization fields of the National Centers for Environmental Prediction (NCEP) Rapid Update Cycle (RUC) model.

The location and magnitude of the central low pressure, the overall general pattern of reflectivity, the values

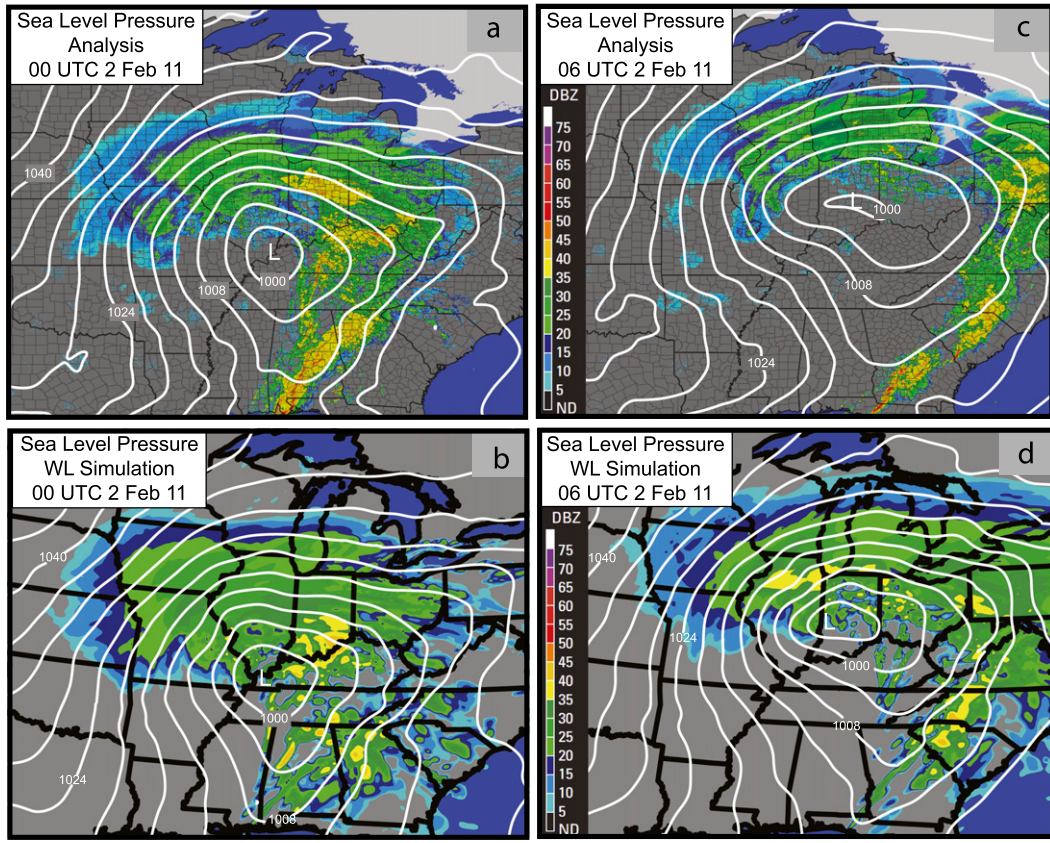


FIG. 3. The 2 Feb 2011 sea level pressure (hPa), and composite radar reflectivity (dBZ): observations at (a) 0000 and (c) 0600 UTC; WL simulation at (b) 0000 and (d) 0600 UTC.

of reflectivity in the GL region, and the magnitude of the pressure gradient in the vicinity of the GL were nearly identical at 0000 UTC, 24 h into the WL simulation. During the following 6 h when the heaviest precipitation fell, the cyclone deepened more rapidly in the WL simulation to a central pressure of 995 hPa, while the observed central pressure reduced to 999 hPa. This difference led to a somewhat stronger pressure gradient across Lake Michigan in the simulation late in the storm. At 0600 UTC, the center of the cyclone was located over central Indiana in both the observations and simulation. The general reflectivity pattern and the reflectivity values in the Chicago–Milwaukee corridor were also similar, except just south of Lake Michigan, where the reflectivity in the simulation was about 2–3 dBZ greater.

At 0600 UTC at 850 hPa (Figs. 4c,d), the location of the center of the storm was identical in both the simulation and observations; however, the central geopotential height was about 15 m deeper in the simulation, consistent with the deeper sea level pressure seen in Fig. 3d. Comparing the 300-hPa fields in Figs. 4a and 4b, the difference in storm intensity at 0600 UTC likely was due to enhanced dynamic forcing in the

simulation associated with a slightly stronger jet streak over southern Indiana ( $\sim 85$  vs  $80 \text{ m s}^{-1}$  in the observations). The magnitude and distribution of temperature at 850 hPa was similar in the observations and simulation, particularly over the Milwaukee–Chicago corridor, where the 850-hPa temperature ranged between  $-10^\circ$  to  $-15^\circ\text{C}$  in both the observations and simulations.

Figure 5 compares the simulated and observed total melted equivalent precipitation produced by the cyclone. Precipitation gauge data used to compile Fig. 5a are reported in inches once per day at 0700 local time (LT) and represent 24-h totals. The total storm precipitation in Fig. 5a represents the accumulated precipitation between 0700 LT 31 January and 0700 LT 3 February. The precipitation data were compiled, quality controlled, and contoured in inches by the Midwest Regional Climate Center (MRCC) at the Illinois State Water Survey. There were 1581 snowfall reports within the 9 complete states appearing in Fig. 5, including 290 sites in Illinois, 237 in Wisconsin, and 231 in Michigan. The data were from the National Weather Service Cooperative network and the Community Collaborative Rain, Hail, and Snow (CoCoRaHS) trained

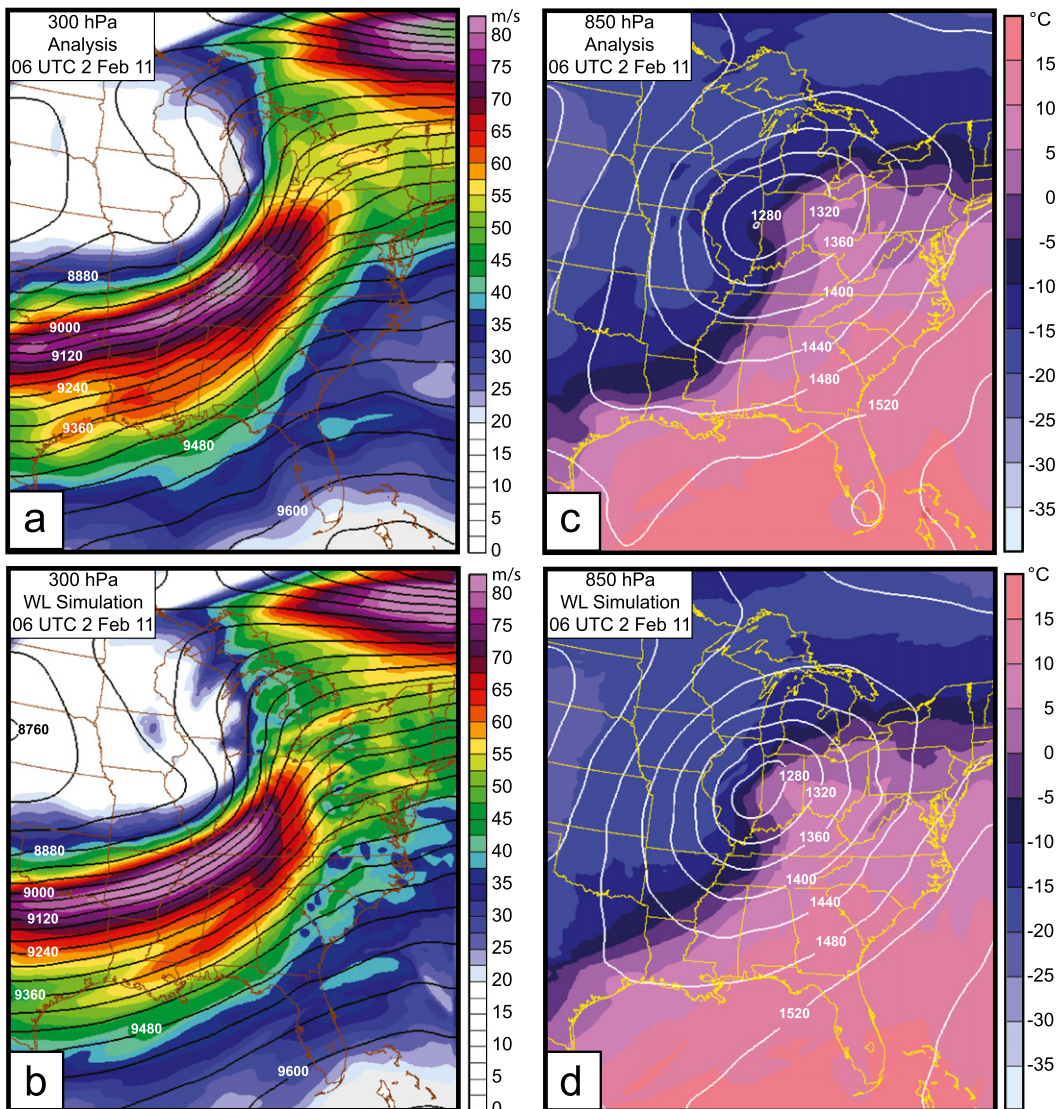


FIG. 4. At 0600 UTC 2 Feb 2011: wind speeds ( $\text{m s}^{-1}$ , shaded) and geopotential height (m, contour, 40-m interval) at 300 hPa from (a) RUC analysis and (b) WL simulation; 850-hPa temperatures ( $^{\circ}\text{C}$ , shaded) and geopotential height (m, contour, 40-m interval) from (c) RUC analysis and (d) WL simulation.

observer network. The original data were interpolated to a  $5\text{ km} \times 5\text{ km}$  grid using the natural neighbor interpolation scheme within the National Center for Atmospheric Research Command Language (NCL) software package. Inches will be used in the comparisons that follow, rather than standard metric measurements, to conform to the MRCC plotting conventions. Note that snow and sleet covered much of the region (see Fig. 1). Problems with precipitation measurements in snowfall due to high winds, gauge capping, poor catchment, snow compaction, and drifting are well known (Rasmussen et al. 2012) and without doubt impacted the accuracy of the measurements used to

compile Fig. 5a. With that uncertainty acknowledged, overall the observations and simulation show good agreement, with the simulation producing slightly greater precipitation in some areas of the domain in Fig. 5. Focusing specifically on the Milwaukee–Chicago corridor, at O’Hare airport, the snow-to-water ratio was observed to be 13.6:1 during this storm. To the degree that the O’Hare measurement characterizes the true snow–water equivalent across the storm, and to the extent that once-per-day measured snow depth across the region characterizes the true snow depth when the snow first fell, a comparison of observed and model snow depth can be made.

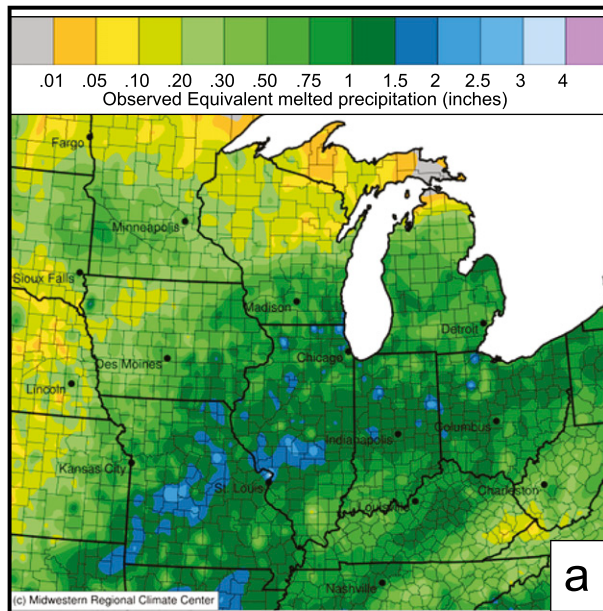
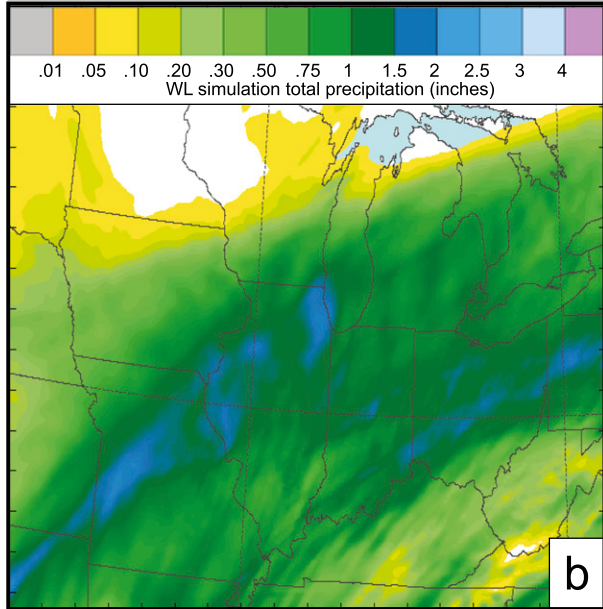
**a**

FIG. 5. Total liquid equivalent precipitation (a) observed during the passage of the 1–2 Feb 2011 cyclone across the GL region and (b) from the WL simulation.

Figure 6, which uses the same MRCC dataset, shows this comparison of total snowfall using the O'Hare airport ratio to convert the simulated precipitation to equivalent snow depth. Within all the uncertainties, the modeled snowfall in the WL control simulation exceeded the snowfall within the downtown Chicago area along the southwest shore of Lake Michigan by about 5–8 in. (12.7–20.3 cm), with the difference reducing to near zero northward along the west shore of Lake Michigan to near Milwaukee.

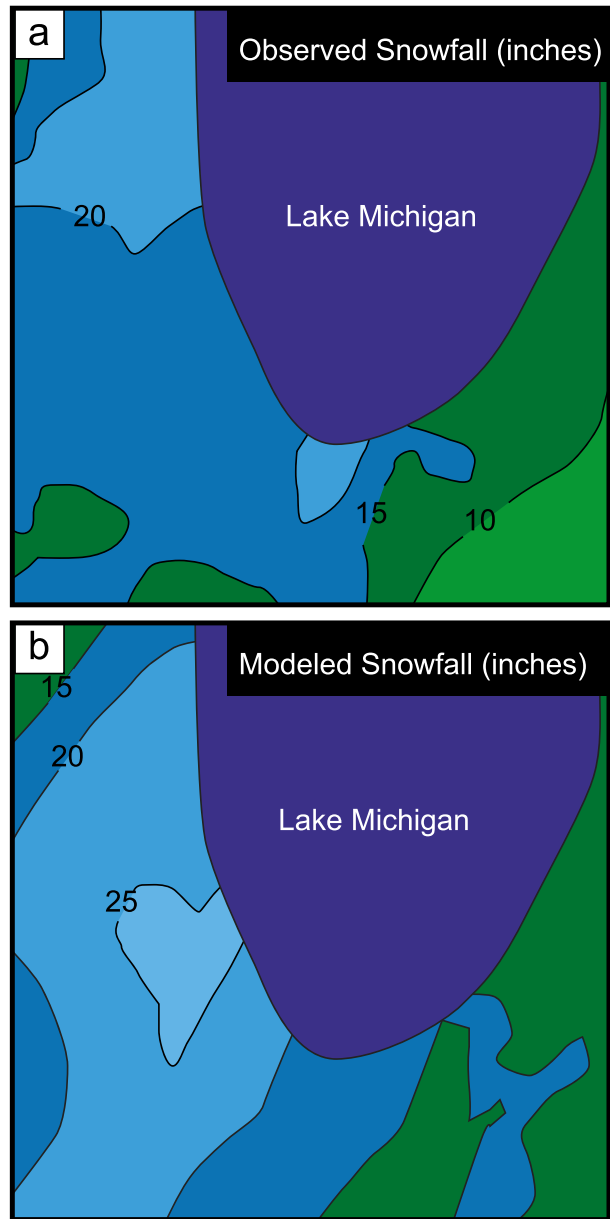


FIG. 6. Storm total snowfall from (a) observations and (b) WL simulation. The simulated snowfall amounts were based on a 13.6:1 conversion between liquid equivalent precipitation and snowfall.

The overall similarity between the evolution of the simulated and actual cyclone provide sufficient evidence that the WL simulation can serve as an adequate control to evaluate the hypothesis stated in section 1, specifically that northeasterly flow across the GL during the 1–2 February cyclone had a significant impact on the extreme snowfall in the Chicago–Milwaukee corridor during this event. In the following section, the WL and NL simulations are compared to assess the degree to which the GL impacted precipitation within the

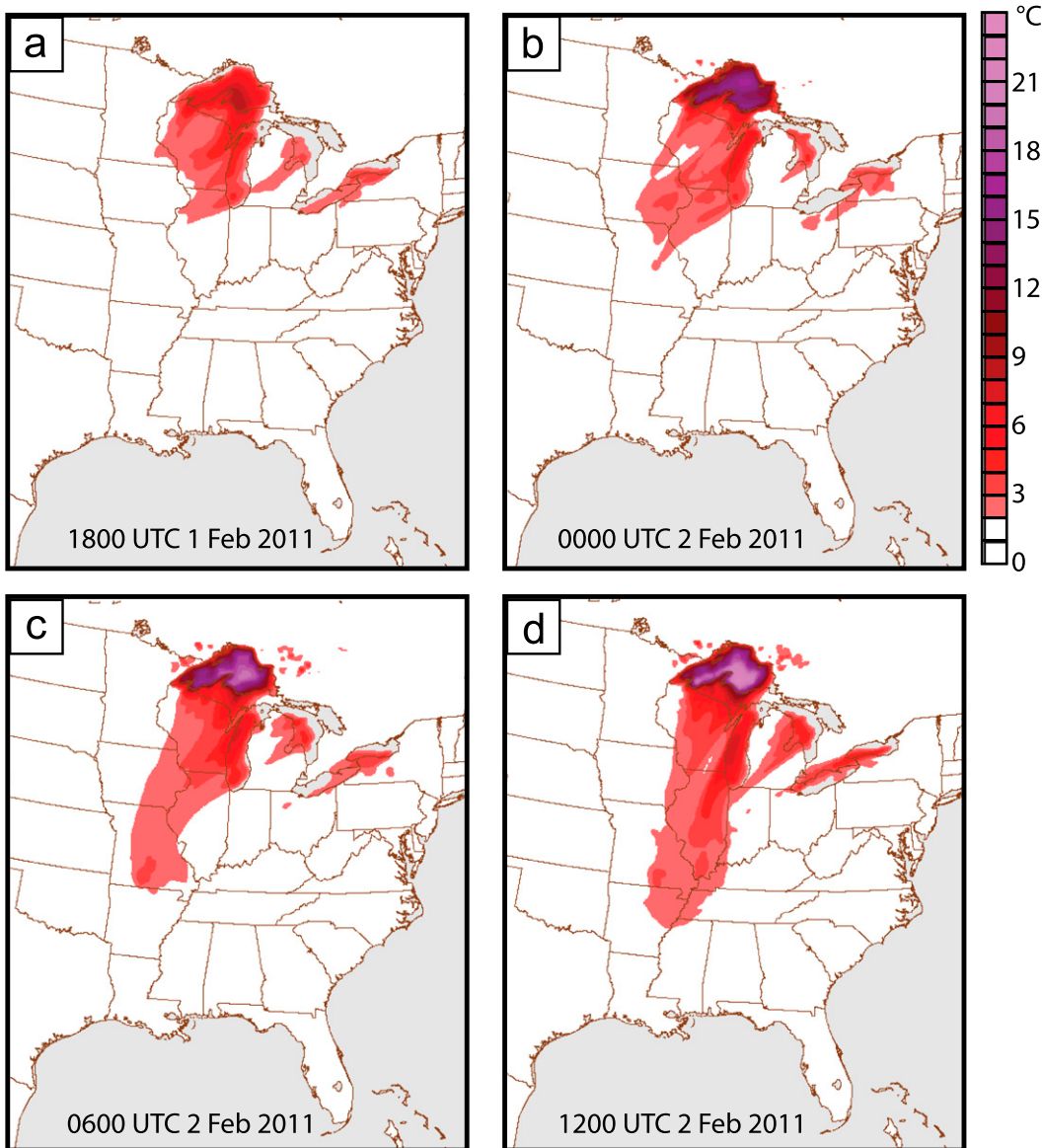


FIG. 7. WL – NL surface temperature difference at four times during the passage of the cyclone.

Chicago–Milwaukee corridor, and evaluate the physical reasons why any differences in precipitation may have occurred.

#### 4. Impact of the Great Lakes

The impact of the GL was examined quantitatively by subtracting fields at equivalent times from the WL and NL simulations. In the figures that follow, difference fields for various quantities are designated as WL–NL. Although the paper's focus is lake-enhanced precipitation in the Chicago–Milwaukee corridor, it is useful to examine the impact of the lakes on

downstream thermal, moisture, and wind fields across a larger region.

##### *a. Impact on thermal, moisture, wind, and pressure fields*

Figure 7 shows the surface temperature difference between the WL and NL simulations at four times during the simulations to illustrate how the thermal plume from the lakes evolved in the model. Plumes of warm air were transported downwind, particularly from Lakes Superior and Michigan, during the WL simulation. By hour +36 of the simulations at 1200 UTC 2 February, the thermal difference plume

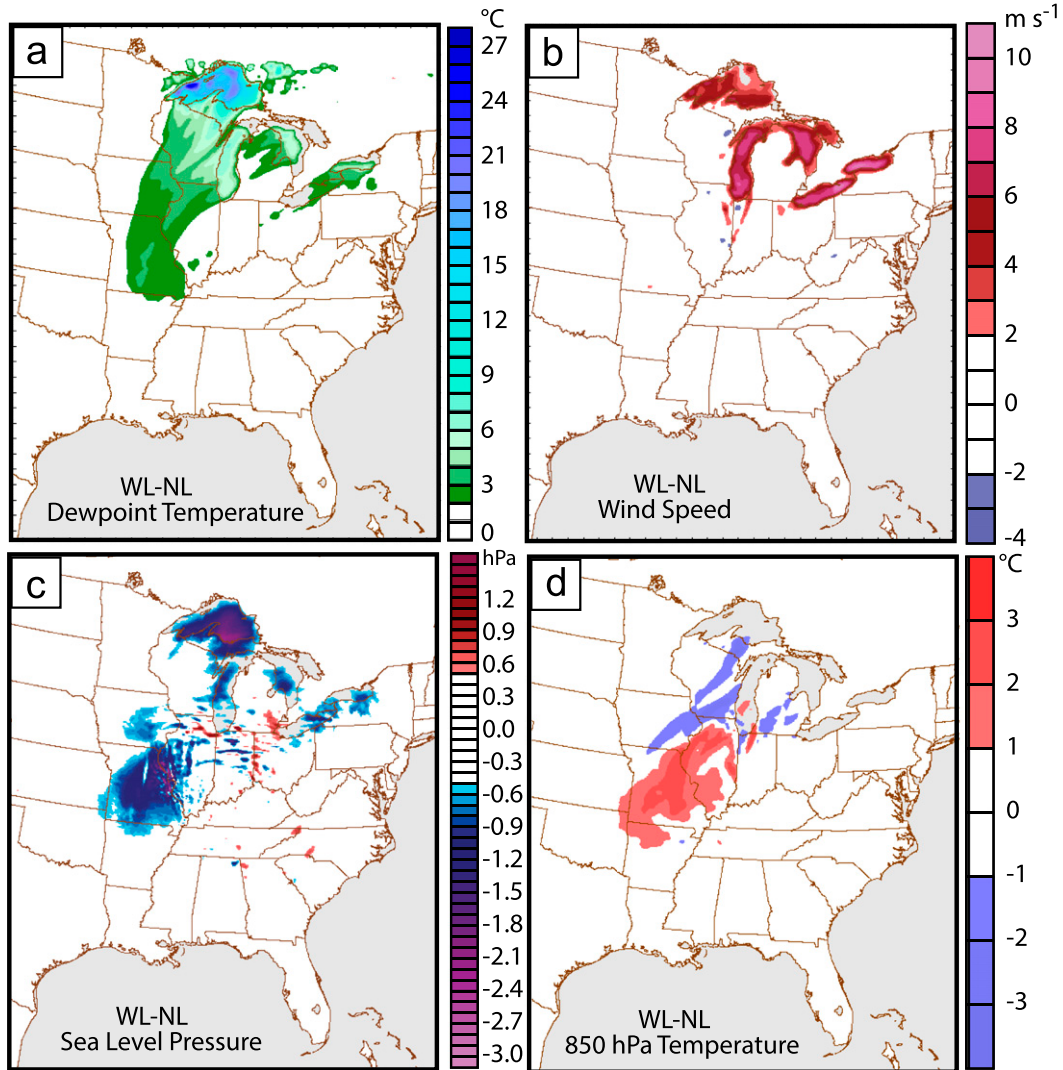


FIG. 8. WL – NL (a) surface dewpoint temperature difference, (b) surface wind speed difference, (c) sea level pressure difference, and (d) 850-hPa temperature difference, at 0600 UTC 2 Feb 2011.

extended several hundred kilometers downwind as far south as northeast Arkansas and northwest Mississippi. The orientation of the plumes' axes shifted from southwestward toward the south over time, following the wind flow around the low pressure center as it moved to the east. The effects of ice cover over part of the eastern lakes in the WL simulation are evident, as the plume from these lakes was minimal (e.g., Vavrus et al. 2013). The temperature change at 0600 UTC induced by the lakes was +3° to +4°C across the Chicago metropolitan region and +5° to +6°C along Lake Michigan's northwest shore closer to Milwaukee. By 1200 UTC 2 February, the WL–NL temperature difference over central Lake Superior reached +22°C and over central Lake Michigan it reached +7° to +9°C.

Dewpoint temperature differences, shown in Fig. 8a for 0600 UTC only, similarly show a moisture plume stretching far downwind of the GL. Lake Superior generated the largest dewpoint difference and affected the largest area. Along the western shore of Lake Michigan, dewpoint temperature changes resulting from the lakes ranged from +3° to +4°C in the vicinity of Chicago to as large as +5° to +6°C along the northwest shore closer to Milwaukee.

Figure 8b shows the surface wind speed changes associated with the lakes at 0600 UTC. Wind speeds were as much as +9 m s<sup>-1</sup> higher over the central parts of Lake Michigan at 0600 UTC, while near the shores the speed increase was 6–7 m s<sup>-1</sup>. However, unlike temperature and dewpoint temperature, changes in wind

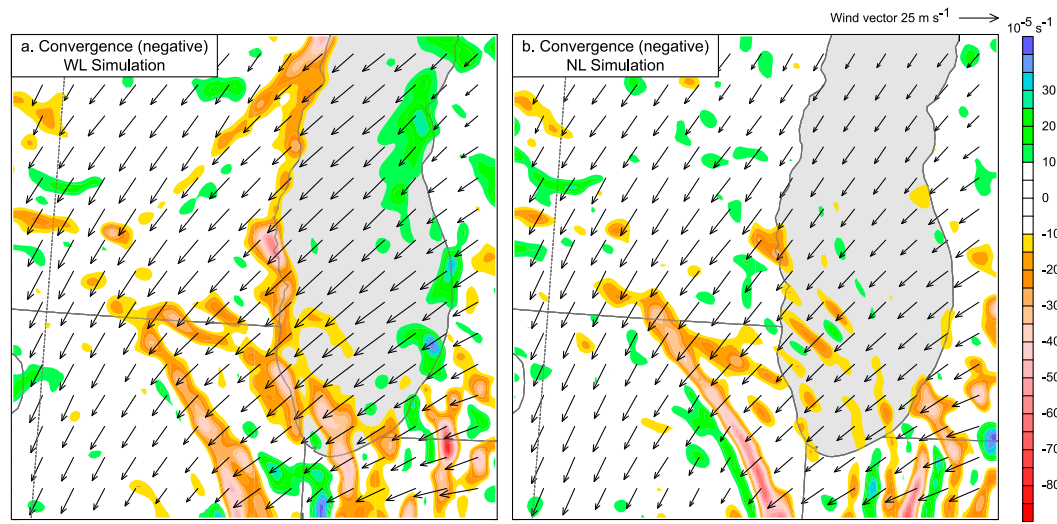


FIG. 9. Surface convergence (negative values) and surface wind vectors at 0600 UTC 2 Feb 2011 from (a) the WL simulation and (b) the NL simulation.

speed were largely confined to the lakes, consistent with less surface drag over water compared to land. Once on shore, airflow in the WL simulation quickly approached values similar to the NL simulation. The

reduction in wind at the western shoreline of Lake Michigan led to a narrow zone of enhanced surface convergence along the lakefront in the WL simulation (Fig. 9).

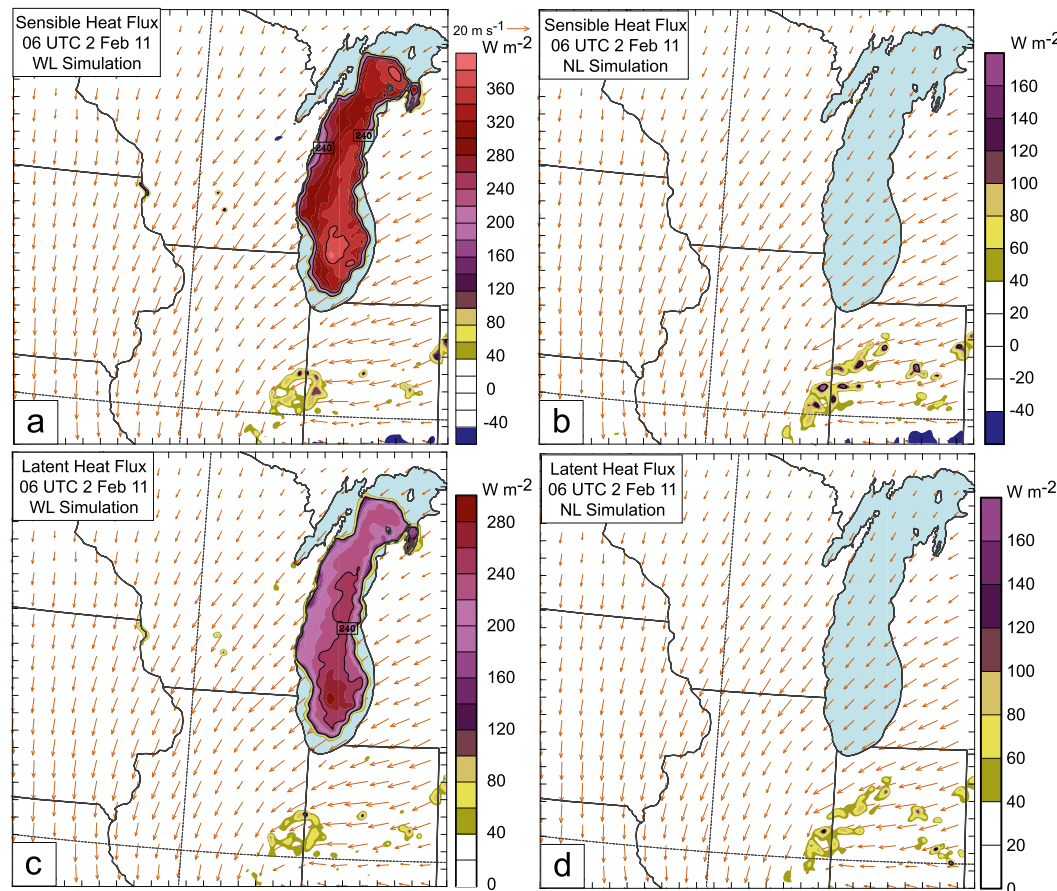


FIG. 10. Surface wind vectors and sensible and latent heat fluxes at 0600 UTC 2 Feb 2011 for the (a),(c) WL and (b),(d) NL simulations.

**Figure 8c** shows the mean sea level pressure (MSLP) changes induced by the GL. Changes initially developed over the GL, but over time, a large area over Missouri and later over Illinois and the lower Mississippi Valley experienced a reduction in MSLP. The downwind pressure differences were at their most intense, between  $-2.0$  and  $-2.5$  hPa, at 0600 UTC in **Fig. 8c** over eastern Missouri and at 1200 UTC over central Illinois and western Indiana. Pressure changes appearing in **Fig. 8c** were associated with warmer air below the frontal inversion in the WL simulation caused by advection of warm air downstream from the GL, based on examination of model soundings in the region of lowest pressure (not shown).

The 850-hPa temperature differences at 0600 UTC (**Fig. 8d**) displayed a more complicated pattern than at the surface. Early in the simulations, temperatures were lower at 850 hPa downwind of Lake Michigan when the lakes were present. Temperature increases developed over Illinois and Missouri due to the lakes by 0000 UTC. Analysis of model soundings showed that the 850-hPa level was within the frontal inversion. The positive and negative temperature changes between the WL and NL simulations near the GL in **Fig. 8d** are attributable to changes in the height of the frontal inversion. Based on examination of model soundings, the lower temperatures at 850 hPa in the WL simulation near the GL were associated with a slight rise in the inversion height at those locations.

**Figure 10** compares the sensible and latent heat fluxes from the WL and NL simulations. As would be expected, the fluxes in the NL simulation were small and equivalent to that from the surrounding land. In the WL simulation, the maximum sensible heat flux,  $380\text{--}400 \text{ W m}^{-2}$ , and latent heat flux,  $260\text{--}300 \text{ W m}^{-2}$ , occurred midlake east of the Chicago–Milwaukee corridor. The sensible heat fluxes over most of Lake Michigan exceeded  $300 \text{ W m}^{-2}$ , while latent heat fluxes exceeded  $200 \text{ W m}^{-2}$ .

#### b. Impact on precipitation

**Figure 11** shows differences in liquid equivalent precipitation between the WL and NL simulation larger than 5 mm, equivalent to 2.7 in. (6.9 cm) of snow. The integration time for the precipitation accumulation started at 2000 UTC 1 February, and ended at 1500 UTC 2 February, the time period where precipitation from the cyclone impacted the major population corridor along the western shore of Lake Michigan.

The only significant difference between the simulations occurred along the southwest shore of Lake Michigan. In this region, maximum precipitation

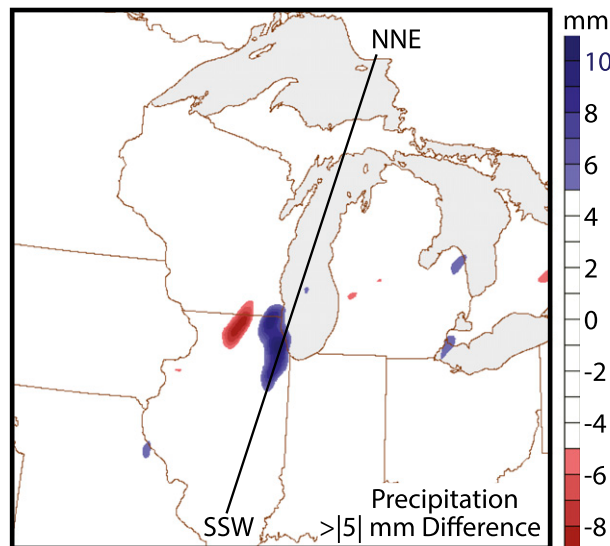


FIG. 11. WL – NL precipitation accumulation difference between 2000 UTC 1 Feb (the time the cyclone's precipitation shield first entered the Great Lakes region) and 1500 UTC 2 Feb (the time the precipitation shield dissipated over Lakes Michigan and Huron). The line denotes the location of the cross sections in **Figs. 12–14**.

accumulations in the WL simulation ranged from 45 to 48 mm, whereas in the NL simulation, the maximum accumulations were 35–38 mm, about a 10-mm difference. Assuming a 13.6:1 ratio of liquid equivalent precipitation to snow depth, the WL simulation predicted snowfall would have been 612–652 mm (24.1–25.7 in.), an overestimate compared to the observed 538 mm (21.2 in.) observed at O'Hare Airport. The snow depth for the NL run, with a 13.6:1 ratio, would have been 476–516 mm (18.7–20.3 in.). These results indicate that at most 21%–23% of the snowfall in the immediate Chicago metropolitan area during this cyclone can be attributed to the presence of the GL. A time series of the precipitation accumulation in the Chicago area showed that most of the WL–NL lake-induced precipitation fell toward the end of the event between 0600 and 1500 UTC. Also notable is the small area along the north-central border of Illinois where the NL simulation produced up to 8 mm more precipitation than the WL simulation. The explanation for this feature is not obvious.

#### c. Impact on boundary layer stability

Cross sections showing potential temperature  $\theta$  and equivalent potential temperature  $\theta_e$  were developed along a line north-northeast (NNE)–south-southwest (SSW) in **Fig. 11** to understand the precipitation distribution changes over the Chicago–Milwaukee corridor in the context of the temperature and moisture changes

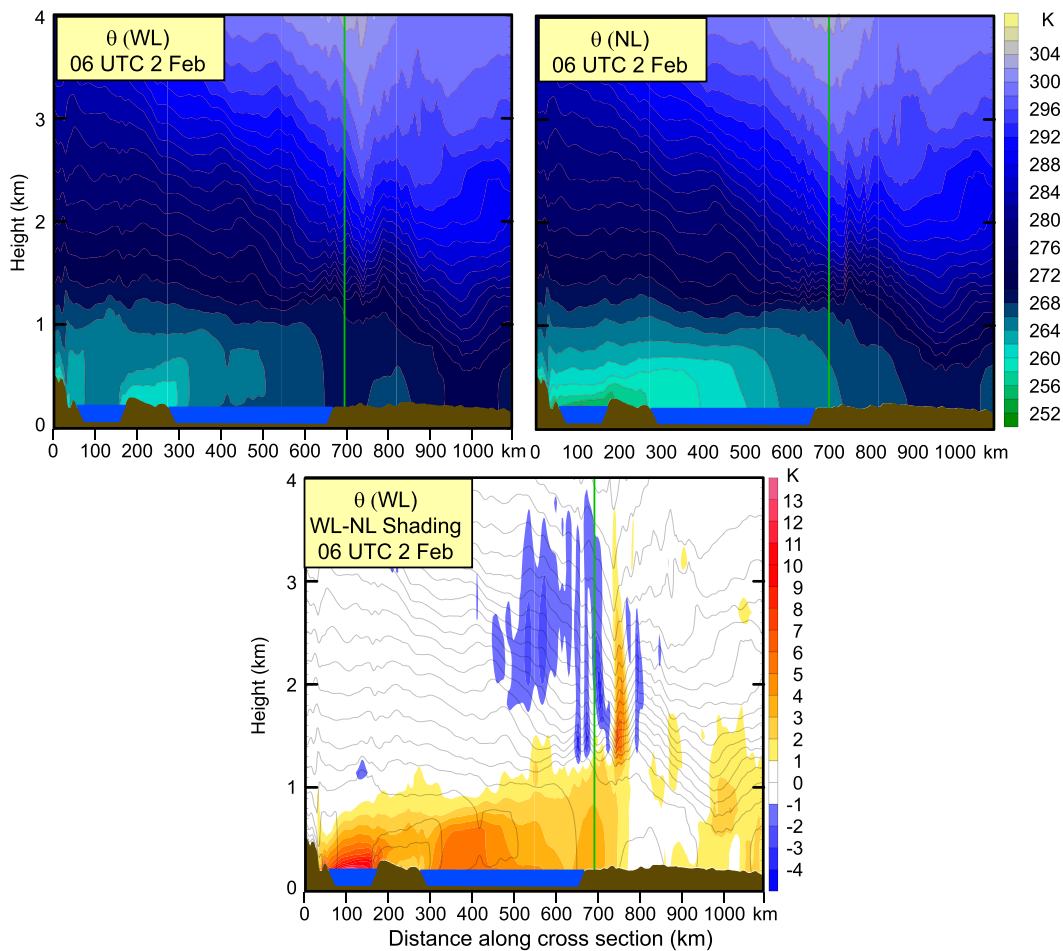


FIG. 12. Cross sections of (a) potential temperature (K) 30 h into the WL simulation at 0600 UTC 2 Feb 2011. (b) As in (a), but for the NL simulation. (c) As in (a), but with shading showing the difference in potential temperature (WL – NL). The location of the cross section is shown in Fig. 11.

associated with the sensible and latent heat fluxes from the GL. The cross section crosses Lake Superior, passes over Lake Michigan near parallel to the lake axis, across the Chicago metropolitan area, and across most of Illinois.

Figure 12 shows  $\theta$  along this cross section for the WL and NL simulations, as well as the difference field superimposed on the  $\theta$  field from the WL simulation. The NL simulation (Fig. 12b) shows the base of the frontal inversion at about 1.2 km MSL. The surface-based cold air mass is shallow, with  $\theta$  increasing uniformly from NNE to SSW. The lapse rates are such that  $d\theta/dz > 0$  within the boundary layer. In the WL simulation (Fig. 12a), warmer air extends higher over the lakes region and  $d\theta/dz = 0$  over the lakes. There is even evidence of superadiabatic lapse rates very close to the lake surface. The difference field in Fig. 12c shows the impact of the lakes. Over Lake Superior, the surface

$\theta$  was as much as 10–11 K higher in the WL simulation compared to the NL simulation. At the surface over Lake Michigan, the WL–NL difference was 5–6 K. Figure 12c shows that convective mixing within the cold air mass over the lakes due to heating by the lakes warmed air between 1 and 6 K, with the largest change at the surface and the least at the base of the frontal inversion. The boundary layer convection (inferred from  $d\theta/dz$  in Fig. 12c) and surface convergence at the downstream end of Lake Michigan (inferred from wind speed changes at the lake–shore boundary in Fig. 9) led to perturbations of the inversion and small-scale vertical fluctuations in the  $\theta$  difference field. These fluctuations were associated with  $\sim$ 1–2-K changes in  $\theta$  above the inversion.

Figure 13 shows the  $\theta_e$  field in the same format as in Fig. 12. As expected based on the  $\theta$  field,  $d\theta_e/dz$  is negative directly above the lake surface in the WL

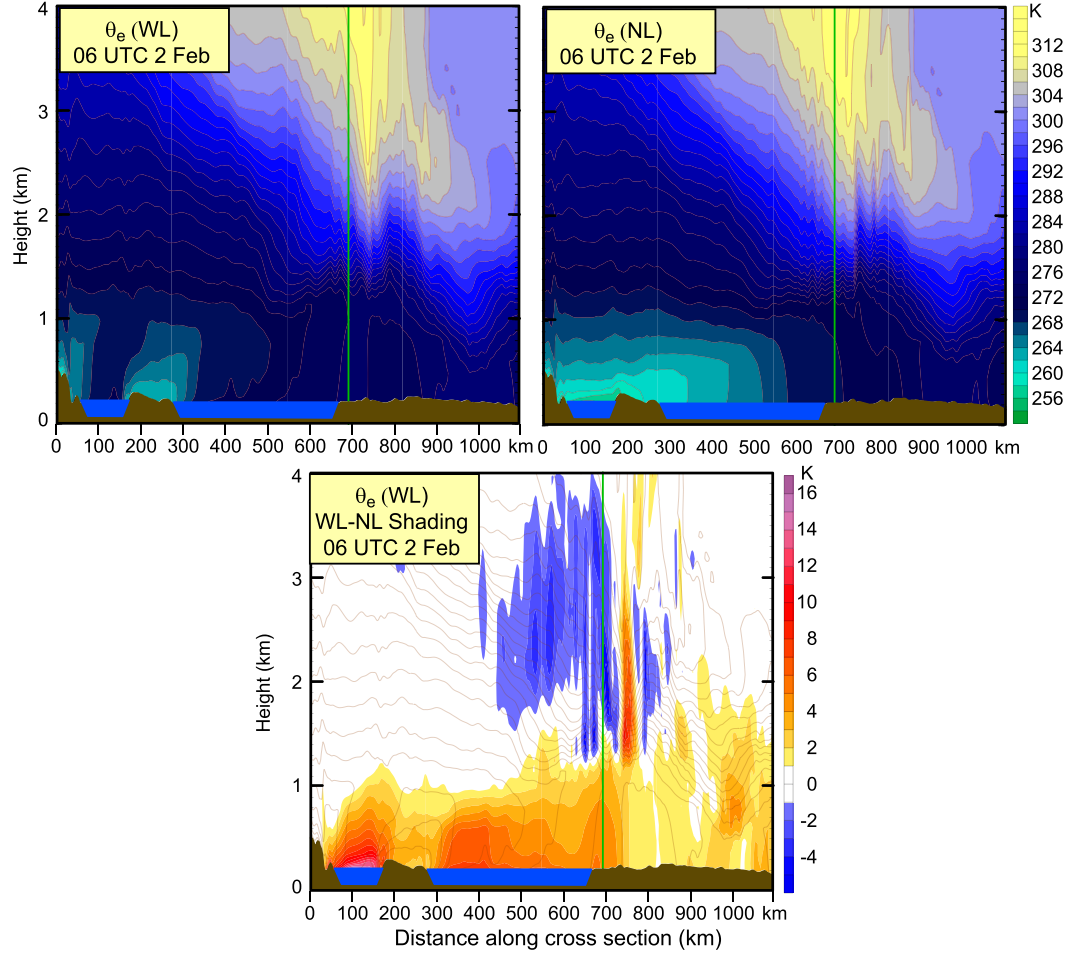


FIG. 13. Cross sections of (a) equivalent potential temperature (K) 30 h into the WL simulation at 0600 UTC 2 Feb 2011. (b) As in (a), but for the NL simulation. (c) As in (a), but with shading showing the difference in equivalent potential temperature (WL – NL). The location of the cross section is shown in Fig. 11. The vertical green line shows the location of Chicago.

simulation. The lakes led to increases in  $\theta_e$  of 8–11 K over Lake Superior and 5–7 K over Lake Michigan, with  $\theta_e$  increases extending to the base of the frontal inversion. The equilibrium level for any convection originating over the lakes was the base of the frontal inversion, limiting lake-induced convection to a depth of about 1.2 km. Downwind of the GL over Illinois, the boundary layer was even shallower, so the potential of lake-induced convective clouds to produce precipitation was limited by the shallow nature of any convective clouds that might develop. The capping of the lake-induced convection by the frontal inversion appears to be the reason why accumulated precipitation  $>5$  mm induced by the lakes in the WL simulation was limited to the narrow region over the Chicago metropolitan area.

The evolution of the WL  $\theta$  field, and the  $\theta$  difference field at four times during the evolution of the storm is

shown in Fig. 14. Note the general deepening of the cold surface layer, as well as the progressive differential (WL–NL) warming of the air by the lakes with time as the cyclone evolved. The deepening of the layer below the frontal inversion in the WL simulation combined with the heat provided by the lake favored sufficiently deep convection later in the simulation to create lake-induced precipitation along the downwind shore in the Chicago region, particularly between 0600 and 1500 UTC when the largest WL–NL differences in precipitation occurred in the simulations.

## 5. Summary

The impact of the GL on the duration, intensity, and organization of snowfall in their lee during cold air outbreaks has been the subject of investigations for

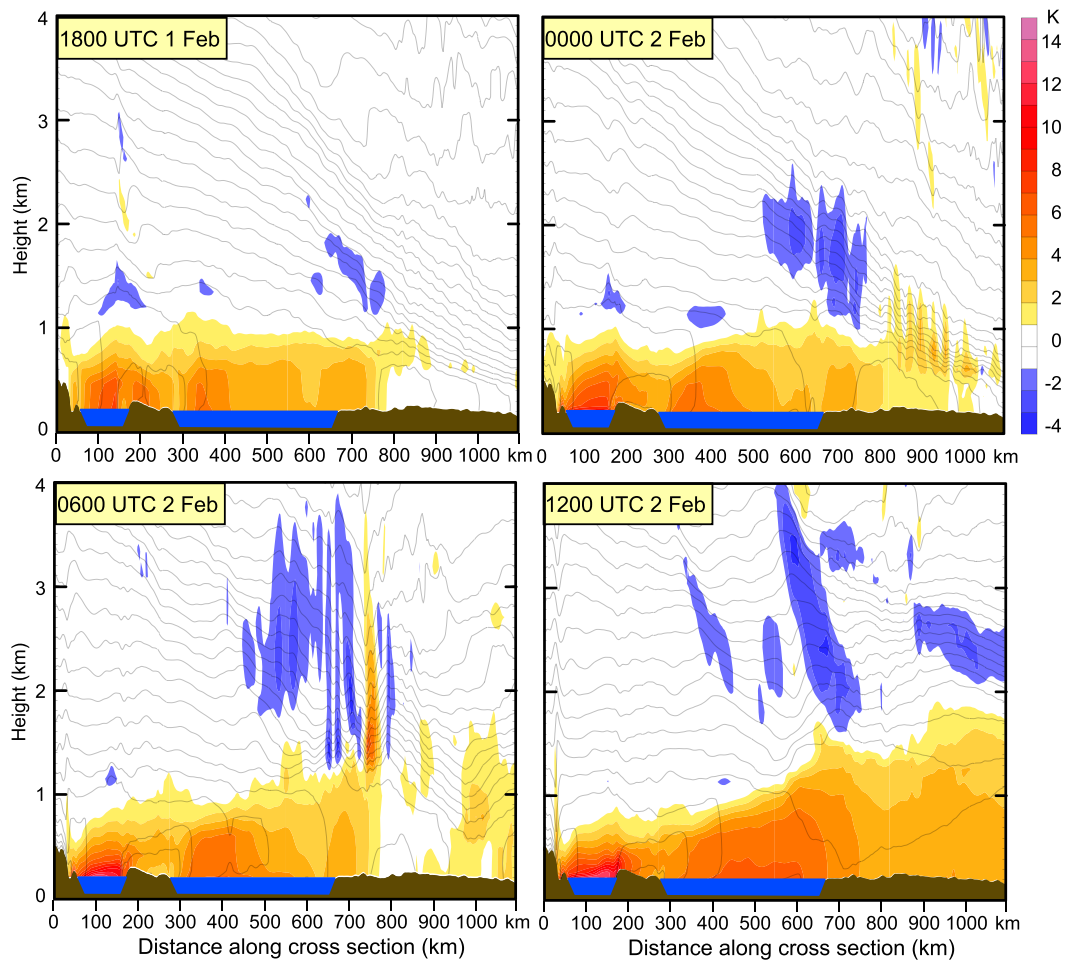


FIG. 14. Time sequence showing the evolution of the potential temperature field (contours) for the WL simulation, and the difference field (colors, WL – NL) at four times during the simulated storm. The location of the cross section is shown in Fig. 11.

over a half century (e.g., Wiggins 1950; Peace and Sykes 1966; Hjelmfelt and Braham 1983; Norton and Bolsenga 1993; Barthold and Kristovich 2011; Veals and Steenburgh 2015; Campbell et al. 2016). The role the GL play in modifying the precipitation distribution during the passage of a cyclone, particularly one responsible for heavy snowfall across the GL region, is less well understood. In this paper, the impact of the GL on the precipitation across a major metropolitan area, the Chicago–Milwaukee corridor, was addressed with numerical simulations using the approach first pioneered by Danard and Rao (1972) of comparing two simulations: one with the lakes present and the other with the lakes replaced with characteristics of the surrounding land. The approach of examining the WL–NL simulation differences revealed several features.

The GL altered the surface temperature and moisture fields in their lee during cyclone passage. These changes

were limited to the layer below the frontal inversion, but were significant enough to reduce the MSLP by 2.0–2.5 hPa, and raise the surface temperature and dewpoint temperature by 2°–4°C across several states downwind. Beyond these changes, the impact of the GL on the overall larger-scale cyclone structure was insignificant, confirming previous findings by Sousounis and Fritsch (1994).

Locally, in the Chicago–Milwaukee metropolitan corridor where the heaviest snow occurred, the surface temperature and dewpoint temperature increased +3°–6°C as a result of heating and moistening of the atmosphere due to surface latent and sensible heat fluxes by the GL. Despite these changes, the impact on areal precipitation was surprisingly small, with significant impacts limited to a small area over metropolitan Chicago late in the storm. The reason for the limited impact appeared to be the shallow nature of the cold air mass below the frontal

inversion. Although the lakes clearly destabilized the air, enhanced convergence was limited to a narrow zone along the lake front, and the depth to which convection could penetrate was limited by the frontal inversion to approximately 1 km. These shallow clouds initially had a small impact on the precipitation field. As the storm evolved and the depth of the cold air increased, lake-enhanced precipitation became possible, although it was still confined to a narrow region over metropolitan Chicago. Nevertheless, within this region, about 20% of the snowfall could be attributed to the presence of the GL.

Extreme snowstorms, with snowfall exceeding 40 cm (~15 in.), are rare events in Chicago, happening on average less than once a decade (although two have occurred in the last 5 years). Understanding how the Great Lakes may influence these storms is important for forecasting their severity. This paper addressed this question for one such event. How representative the results are for other extreme events, or for more typical cyclones that produce smaller snowfall totals, remains an open question for future research.

**Acknowledgments.** The composite radar analyses appearing in Figs. 3a and 3c were provided by the Iowa Environmental Mesonet maintained by the Iowa State University Department of Agronomy. We thank Dr. Jim Angel and the Midwest Regional Climate Center at the Illinois State Water Survey for the precipitation analyses in Figs. 1, 5a, and 6. Funding for this research was provided by NSF Grant AGS-1247404 to the University of Illinois.

## REFERENCES

- Angel, J. R., and S. A. Isard, 1997: An observational study of the influence of the Great Lakes on the speed and intensity of passing cyclones. *Mon. Wea. Rev.*, **125**, 2228–2237, doi:[10.1175/1520-0493\(1997\)125<2228:AOSOTI>2.0.CO;2](https://doi.org/10.1175/1520-0493(1997)125<2228:AOSOTI>2.0.CO;2).
- Barthold, F. E., and D. A. R. Kristovich, 2011: Observations of the cross-lake cloud and snow evolution in a lake-effect snow event. *Mon. Wea. Rev.*, **139**, 2386–2398, doi:[10.1175/MWR-D-10-05001.1](https://doi.org/10.1175/MWR-D-10-05001.1).
- Campbell, L. S., W. J. Steenburgh, P. G. Veals, T. W. Letcher, and J. R. Minder, 2016: Lake-effect mode and precipitation enhancement over the Tug Hill Plateau during OWLeS IOP2b. *Mon. Wea. Rev.*, **144**, 1729–1748, doi:[10.1175/MWR-D-15-0412.1](https://doi.org/10.1175/MWR-D-15-0412.1).
- Chen, F., and J. Dudhia, 2001: Coupling an advanced land surface-hydrology model with the Penn State–NCAR MM5 modeling system. Part I: Model implementation and sensitivity. *Mon. Wea. Rev.*, **129**, 569–585, doi:[10.1175/1520-0493\(2001\)129<0569:CAALSH>2.0.CO;2](https://doi.org/10.1175/1520-0493(2001)129<0569:CAALSH>2.0.CO;2).
- Cordeira, J. M., and N. F. Laird, 2008: The influence of ice cover on two lake-effect snow events over Lake Erie. *Mon. Wea. Rev.*, **136**, 2747–2763, doi:[10.1175/2007MWR2310.1](https://doi.org/10.1175/2007MWR2310.1).
- Cox, H. J., 1917: Influence of the Great Lakes upon movement of high and low pressure areas. *Proceedings of the Second Pan-American Science Congress*, Vol. 2 (No. 2), U.S. Government Printing Office, 432–459.
- Danard, M. B., and G. V. Rao, 1972: Numerical study of the effects of the Great Lakes on a winter cyclone. *Mon. Wea. Rev.*, **100**, 374–382, doi:[10.1175/1520-0493\(1972\)100<0374:NSOTEQ>2.3.CO;2](https://doi.org/10.1175/1520-0493(1972)100<0374:NSOTEQ>2.3.CO;2).
- , and A. C. McMillan, 1974: Further numerical studies of the effects of the Great Lakes on winter cyclones. *Mon. Wea. Rev.*, **102**, 166–175, doi:[10.1175/1520-0493\(1974\)102<0166:FNSOTEQ>2.0.CO;2](https://doi.org/10.1175/1520-0493(1974)102<0166:FNSOTEQ>2.0.CO;2).
- Gerbush, M., D. A. R. Kristovich, and N. F. Laird, 2008: Mesoscale boundary layer and heat flux variations over pack ice-covered Lake Erie. *J. Appl. Meteor. Climatol.*, **47**, 668–682, doi:[10.1175/2007JAMC1479.1](https://doi.org/10.1175/2007JAMC1479.1).
- Hjelmfelt, M. R., and R. R. Braham Jr., 1983: Numerical simulation of the airflow over Lake Michigan for a major lake-effect snow event. *Mon. Wea. Rev.*, **111**, 205–219, doi:[10.1175/1520-0493\(1983\)111<0205:NSOTAO>2.0.CO;2](https://doi.org/10.1175/1520-0493(1983)111<0205:NSOTAO>2.0.CO;2).
- Hong, S.-Y., Y. Noh, and J. Dudhia, 2006: A new vertical diffusion package with an explicit treatment of entrainment processes. *Mon. Wea. Rev.*, **134**, 2318–2341, doi:[10.1175/MWR3199.1](https://doi.org/10.1175/MWR3199.1).
- Iacono, M., J. S. Delamere, E. J. Mlawer, M. W. Shephard, S. A. Clough, and W. D. Collins, 2008: Radiative forcing by long-lived greenhouse gases: Calculations with the AER radiative transfer models. *J. Geophys. Res.*, **113**, D13103, doi:[10.1029/2008JD009944](https://doi.org/10.1029/2008JD009944).
- Ikeda, K., M. Steiner, J. Pinto, and C. A. Alexander, 2013: Evaluation of cold-season precipitation forecasts generated by the hourly updating High-Resolution Rapid Refresh model. *Wea. Forecasting*, **28**, 921–939, doi:[10.1175/WAF-D-12-00085.1](https://doi.org/10.1175/WAF-D-12-00085.1).
- Jiménez, P. A., J. Dudhia, J. F. González-Rouco, J. Navarro, J. P. Montávez, and E. García-Bustamante, 2012: A revised scheme for the WRF surface layer formulation. *Mon. Wea. Rev.*, **140**, 898–918, doi:[10.1175/MWR-D-11-00056.1](https://doi.org/10.1175/MWR-D-11-00056.1).
- Morrison, H., G. Thompson, and V. Tatarskii, 2009: Impact of cloud microphysics on the development of trailing stratiform precipitation in a simulated squall line: Comparison of one- and two-moment schemes. *Mon. Wea. Rev.*, **137**, 991–1007, doi:[10.1175/2008MWR2556.1](https://doi.org/10.1175/2008MWR2556.1).
- National Weather Service, 2015: Historic winter storm of January 31–February 2, 2015. National Weather Service, accessed February 2017. [Available online at [http://www.weather.gov/lot/2015\\_Feb01\\_Snow](http://www.weather.gov/lot/2015_Feb01_Snow).]
- Neralla, V. R., and M. B. Danard, 1975: Incorporation of parameterized convection in the synoptic study of large scale effects of the Great Lakes. *Mon. Wea. Rev.*, **103**, 388–405, doi:[10.1175/1520-0493\(1975\)103<0388:IOPCIT>2.0.CO;2](https://doi.org/10.1175/1520-0493(1975)103<0388:IOPCIT>2.0.CO;2).
- Norton, D. C., and S. J. Bolsenga, 1993: Spatiotemporal trends in lake effect and continental snowfall in the Laurentian Great Lakes, 1951–1980. *J. Climate*, **6**, 1943–1956, doi:[10.1175/1520-0442\(1993\)006<1943:STILEA>2.0.CO;2](https://doi.org/10.1175/1520-0442(1993)006<1943:STILEA>2.0.CO;2).
- Notaro, M., K. Holman, A. Zarrin, E. Fluck, S. Vavrus, and V. Bennington, 2013: Influence of the Laurentian Great Lakes on regional climate. *J. Climate*, **26**, 789–804, doi:[10.1175/JCLI-D-12-00140.1](https://doi.org/10.1175/JCLI-D-12-00140.1).
- Owens, N., 2016: The role of lake enhancement in the evolution of the 2011 Chicago-area Groundhog's Day blizzard. M.S. thesis, Dept. of Atmospheric Sciences, University of Illinois at Urbana–Champaign, Urbana, IL, 56 pp.
- Peace, R. L., Jr., and R. B. Sykes Jr., 1966: Mesoscale study of a lake effect snow storm. *Mon. Wea. Rev.*, **94**, 495–507, doi:[10.1175/1520-0493\(1966\)094<0495:MSOALE>2.3.CO;2](https://doi.org/10.1175/1520-0493(1966)094<0495:MSOALE>2.3.CO;2).

- Petterssen, S., 1956: *Motion and Motion Systems*. Vol. I, *Weather Analysis and Forecasting*, McGraw-Hill, 428 pp.
- , and P. A. Calabrese, 1959: On some weather influences due to warming of the air by the Great Lakes in winter. *J. Meteor.*, **16**, 646–652, doi:[10.1175/1520-0469\(1959\)016<0646:OSWIDT>2.0.CO;2](https://doi.org/10.1175/1520-0469(1959)016<0646:OSWIDT>2.0.CO;2).
- Rasmussen, R., and Coauthors, 2012: How well are we measuring snow: The NOAA/FAA/NCAR winter precipitation test bed. *Bull. Amer. Meteor. Soc.*, **93**, 811–829, doi:[10.1175/BAMS-D-11-00052.1](https://doi.org/10.1175/BAMS-D-11-00052.1).
- Rauber, R. M., and Coauthors, 2014: Stability and charging characteristics of the comma-head region of continental winter cyclones. *J. Atmos. Sci.*, **71**, 1559–1582, doi:[10.1175/JAS-D-13-0253.1](https://doi.org/10.1175/JAS-D-13-0253.1).
- Sousounis, P. J., 1997: Lake-aggregate mesoscale disturbances. Part III: Description of a mesoscale aggregate vortex. *Mon. Wea. Rev.*, **125**, 1111–1134, doi:[10.1175/1520-0493\(1997\)125<1111:LAMDP>2.0.CO;2](https://doi.org/10.1175/1520-0493(1997)125<1111:LAMDP>2.0.CO;2).
- , 1998: Lake-aggregate mesoscale disturbances. Part IV: Development of a mesoscale aggregate vortex. *Mon. Wea. Rev.*, **126**, 3169–3188, doi:[10.1175/1520-0493\(1998\)126<3169:LAMDP>2.0.CO;2](https://doi.org/10.1175/1520-0493(1998)126<3169:LAMDP>2.0.CO;2).
- , and H. N. Shirer, 1992: Lake aggregate mesoscale disturbances. Part I: Linear analysis. *J. Atmos. Sci.*, **49**, 80–96, doi:[10.1175/1520-0469\(1992\)049<0080:LAMDP>2.0.CO;2](https://doi.org/10.1175/1520-0469(1992)049<0080:LAMDP>2.0.CO;2).
- , and J. M. Fritsch, 1994: Lake-aggregate mesoscale disturbances. Part II: A case study of the effects on regional and synoptic-scale weather systems. *Bull. Amer. Meteor. Soc.*, **75**, 1793–1811, doi:[10.1175/1520-0477\(1994\)075<1793:LAMDP>2.0.CO;2](https://doi.org/10.1175/1520-0477(1994)075<1793:LAMDP>2.0.CO;2).
- , and G. E. Mann, 2000: Lake-aggregate mesoscale disturbances. Part V: Impacts on lake-effect precipitation. *Mon. Wea. Rev.*, **128**, 728–745, doi:[10.1175/1520-0493\(2000\)128<0728:LAMDP>2.0.CO;2](https://doi.org/10.1175/1520-0493(2000)128<0728:LAMDP>2.0.CO;2).
- Thompson, G., and T. Eidhammer, 2014: A study of aerosol impacts on clouds and precipitation development in a large winter cyclone. *J. Atmos. Sci.*, **71**, 3636–3658, doi:[10.1175/JAS-D-13-0305.1](https://doi.org/10.1175/JAS-D-13-0305.1).
- Vavrus, S., M. Notaro, and A. Zarrin, 2013: The role of ice cover in heavy lake-effect snowstorms over the Great Lakes basin as simulated by RegCM4. *Mon. Wea. Rev.*, **141**, 148–165, doi:[10.1175/MWR-D-12-00107.1](https://doi.org/10.1175/MWR-D-12-00107.1).
- Veals, P. V., and W. J. Steenburgh, 2015: Climatological characteristics and orographic enhancement of lake-effect precipitation east of Lake Ontario and over the Tug Hill Plateau. *Mon. Wea. Rev.*, **143**, 3591–3609, doi:[10.1175/MWR-D-15-0009.1](https://doi.org/10.1175/MWR-D-15-0009.1).
- Warner, T. A., T. L. Lang, and W. A. Lyons, 2014: Synoptic scale outbreak of self-initiated upward lightning (SIUL) from tall structures during the central U.S. blizzard of 1–2 February 2011. *J. Geophys. Res. Atmos.*, **119**, 9530–9548, doi:[10.1002/2014JD021691](https://doi.org/10.1002/2014JD021691).
- Wiggin, B. L., 1950: Great snows of the Great Lakes. *Weatherwise*, **3**, 123–126, doi:[10.1080/00431672.1950.9927065](https://doi.org/10.1080/00431672.1950.9927065).
- Wright, D. M., D. J. Posselt, and A. L. Steiner, 2013: Sensitivity of lake-effect snowfall to lake ice cover and temperature in the Great Lakes region. *Mon. Wea. Rev.*, **141**, 670–689, doi:[10.1175/MWR-D-12-00038.1](https://doi.org/10.1175/MWR-D-12-00038.1).